



# The correlation of cathodic peak potentials of vitamin K<sub>3</sub> derivatives and their calculated electron affinities

## The role of hydrogen bonding and conformational changes<sup>☆</sup>

Hamid Reza Nasiri<sup>a,1</sup>, Robin Panisch<sup>b</sup>, M. Gregor Madej<sup>c</sup>, Jan W. Bats<sup>d</sup>,  
C. Roy D. Lancaster<sup>c,2</sup>, Harald Schwalbe<sup>a,\*</sup>

<sup>a</sup> Institute of Organic Chemistry and Chemical Biology, Center for Biomolecular Magnetic Resonance (BMRZ), Johann Wolfgang Goethe-University Frankfurt, Max-von-Laue-Str. 7, D-60438 Frankfurt am Main, Germany

<sup>b</sup> Institute for Pure and Applied Chemistry, Carl-von-Ossietzky-University Oldenburg, Carl-von-Ossietzky-Str. 9-11, D 26129 Oldenburg, Germany

<sup>c</sup> Max Planck Institute of Biophysics, Department Molecular Membrane Biology, Max-von-Laue-Str. 3, D-60438 Frankfurt am Main, Germany

<sup>d</sup> Institute of Organic Chemistry and Chemical Biology, Johann Wolfgang Goethe-University Frankfurt, Max-von-Laue-Str. 7, D-60438 Frankfurt am Main, Germany

### ARTICLE INFO

#### Article history:

Received 12 December 2008

Received in revised form 16 February 2009

Accepted 17 February 2009

Available online 3 March 2009

#### Keywords:

Vitamin K<sub>3</sub> derivatives

Cofactor–protein interactions

Electron affinity  $E_A$

Hydrogen bonding

DFT-calculations

One-electron-transfer reaction

### ABSTRACT

2-methyl-1,4-naphthoquinone **1** (vitamin K<sub>3</sub>, menadione) derivatives with different substituents at the 3-position were synthesized to tune their electrochemical properties. The thermodynamic midpoint potential ( $E_{1/2}$ ) of the naphthoquinone derivatives yielding a semi radical naphthoquinone anion were measured by cyclic voltammetry in the aprotic solvent dimethoxyethane (DME). Using quantum chemical methods, a clear correlation was found between the thermodynamic midpoint potentials and the calculated electron affinities ( $E_A$ ). Comparison of calculated and experimental values allowed delineation of additional factors such as the conformational dependence of quinone substituents and hydrogen bonding which can influence the electron affinities ( $E_A$ ) of the quinone. This information can be used as a model to gain insight into enzyme–cofactor interactions, particularly for enzyme quinone binding modes and the electrochemical adjustment of the quinone motif.

© 2009 Elsevier B.V. All rights reserved.

### 1. Introduction

The quinone scaffold is commonly found within numerous natural products and prosthetic groups [1]. They are known for their anti-inflammatory, anti-tumor, anti-parasitic and anti-microbial activities [2,3]. Quinones are involved in a variety of important cellular functions such as energy transduction [4] and redox cycling [5]. Beside other prosthetic groups such as flavin adenine dinucleotide (FAD), iron–sulfur clusters and heme molecules, quinones act as cofactors for electron transfer between different redox enzymes inside the respiratory complexes located in the membranes of mitochondria, bacteria and chloroplasts. Up to now, structural data on a large number of quinone–enzyme complexes has been reported. Examples

include the ubiquinone in the Q<sub>B</sub> binding pocket of the photosynthetic reaction center [6], ubiquinone in succinate dehydrogenase [7] and also in the Q<sub>i</sub> site of the bc<sub>1</sub> complex [8]. However, in spite of the vast amount of information known about the mode and environment in which quinones bind, comparatively little is known about the binding and redox properties in quinone converting enzymes [9]. The electrochemical properties of quinones are based on their ability to accept one or two electrons to form the radical anion or dianion species respectively. Examples for both processes have been found *in vivo*, the enzyme NADH:cytochrome P-450 reductase is a one-electron-reduction enzyme which produce a semiquinone radical intermediate, while the enzyme NAD(P)H:oxidoreductase is a two-electron-reduction enzyme [10].

The two-electron reduction followed by protonation (quinone/quinol system) is important for the anti-tumor behavior of quinone drugs. Here, quinone-based drugs undergo reductive arylation resulting in DNA cross-linking [11,12]. The one-electron reduction (quinone/semiquinone system) results in the formation of a highly reactive semiquinone radical anion which is able to transfer a single electron to molecular oxygen causing reactive oxygen species (ROS) and oxidative stress. Cytotoxicity is highly dependent on the electrochemical potential of the radical anion produced [5] and affected by mutations in the enzyme's amino acid residues that are

<sup>☆</sup> Electronic Supplementary Information (ESI) available: [cyclic voltammogram of **9**, concentration dependence of the redox potentials for quinones **2** and **6** and their reversibility, differential pulse voltammograms of **4** and **6**, the vertical electron affinity and the relative energy plotted against the conformation of the R group at C3].

\* Corresponding author. Tel.: +496979829737; fax: +496979829515.

E-mail address: [schwalbe@nmr.uni-frankfurt.de](mailto:schwalbe@nmr.uni-frankfurt.de) (H. Schwalbe).

<sup>1</sup> Present address: Department of Chemistry, University of Cambridge, Lensfield Road, Cambridge CB2 1EW, UK.

<sup>2</sup> Present address: Department of Structural Biology, Saarland University, Faculty of Medicine, Building 60, D-66421 Homburg, Germany.

involved in electron leakage from the prosthetic groups in the electron-transfer chain. In contrast to the potential of the two-electron reduction in cancer therapy, one-electron reduction has been found to be associated with a range of different diseases [13]. In the key mechanism of electron transfer and proton translocation across the membrane in the cytochrome *bc*<sub>1</sub> complex (protonmotive Q cycle) [14,15], a stable semiradical was identified as an intermediate in the Q<sub>i</sub> site. Electron transfer is bifurcated and proceeds through a quinol oxidation in the Q<sub>o</sub> site via the low and the high potential b type hemes to the quinone reduction in the Q<sub>i</sub> site. In contrast to the semiquinone radical species formation during the quinone reduction at the Q<sub>i</sub> site, the situation for the quinol oxidation at the Q<sub>o</sub> site remains controversial, particularly with regard to how these enzymes insulate the reactive semiquinone radical from further reaction with oxygen (the so-called bypass reaction [16]) and minimize the decoupling of electron transfer from pumping or formation of superoxide anion. Two models have been proposed to explain this protective behavior (as presented and termed type I and II [17]).

In the “type I” model which is also referred to the “proton-gated affinity change” mechanism, the QH<sub>2</sub> is oxidized by two sequential one-electron transfers, producing a thermodynamically stabilized semiquinone at the Q<sub>o</sub> site via the binding to the “Riske” cluster [18]. In contrast, the “type II” model or the “double-concerted electron-transfer” model involves a concerted two-electron quinone redox chemistry that avoids the semiquinone radical intermediate [19].

In the classical quinone chemistry, however, the *in-vitro* quinone redox reactions can be clearly divided into two categories: the two-electron–two-proton process in water or the one-electron processes in aprotic solvents. The electrochemistry in water shows marked differences in buffered and unbuffered systems [20]. The one-electron reduction involving the formation of a highly reactive semiquinone is an important mechanism, especially in lipophilic environment. Herein, we investigate the electrochemistry of vitamin K<sub>3</sub> (the redox active core of vitamin K) derivatives in aprotic media, where the one-electron-transfer reaction is predominant. Additionally, aprotic solvents mimic the hydrophobic protein interior in which the quinone cofactor is embedded and therefore provide appropriate models for quinone converting enzyme redox behavior.

Recently, substrate analogues of vitamin K with tuned electrochemical behavior [21,22] have been designed to investigate the presence or absence of transmembrane proton transfer in dihem-containing membrane protein complexes based on substrate conversion and specificity. These findings clearly confirmed the correlation of the electrochemical and bioactive properties [23] and particularly the importance of the relative midpoint potential of quinones in relation to cytotoxicity, substrate conversion and specificity. The different redox potential behaviors of quinones are strongly dependent on the substituents of the quinonic or adjacent rings. In the membrane environment, this behavior is tuned by features such as binding orientation, conformational changes and non-covalent interactions such as hydrogen bonding and hydrophobic interactions with protein binding pockets and phospholipids. The role of the protein environment in determining the redox midpoint potential of quinones has been explored using site-directed mutagenesis [24] and FTIR measurements [25].

To verify the different electrochemical effects of substituents of vitamin K<sub>3</sub>, we synthesized a variety of 3-substituted analogues of vitamin K<sub>3</sub>. Their electrochemical behavior was investigated by cyclic voltammetry and correlated to calculated electron affinities determined by density functional calculations. Furthermore, we calculated effects that may help the protein to modulate the electrochemistry of its bond quinone cofactor. Quinones have been a subject of several computational studies [26–31] concerning the structure of the ground state, oxidized and reduced species and spectral properties such as EPR parameters [32,33] and the vibrational spectra [27,34]. The effects

of different substituents at the ring system on the electron affinity and the correlation to experimental results has been extensively investigated for *p*-benzoquinones, but only in part for 1,4-naphthoquinones [35–39]. To the best of our knowledge, there has been no accurate investigation into how the binding of quinones to the target enzyme can affect its electrochemical properties. However, by means of computational chemistry, it is not only possible to partition the total binding energy into contributions arising from substituent effects, conformational changes, and non-covalent interactions such as hydrogen bonding and hydrophobic interactions, but also to investigate their influences on the electrochemistry of quinones in the target protein.

## 2. Materials and methods

### 2.1. General remarks

NMR spectra were recorded at a <sup>1</sup>H frequency of 250 MHz. Elementary analyses were measured on a Foss CHN-O-RAPID instrument. All reactions were monitored by thin-layer chromatography (TLC), performed on silica gel POLYgram® (Macherey-Nagel). Chromatographic purifications were done with Merck silica gel 60.

### 2.2. Computational methods

The structures of the neutral naphthoquinones were initially optimized at the B3LYP level of theory [40], using the 6-31+G(d) basis set. As starting structures for geometry optimization, experimental data obtained from X-ray crystallography were used. The nature of the resulting stationary point was determined by a subsequent frequency calculation. Refined energies were obtained by single-point calculations employing the larger 6-311+G(2d) basis set. Vertical electron affinities were calculated as the difference between the absolute energy of the neutral quinone and the radical anion at the geometry of the neutral quinone. For comparison, adiabatic electron affinities were calculated in a similar manner using the optimized structure of the radical anion. Solvent effects have been introduced using a self consistent reaction field based on the polarizable continuum model (PCM) [41], calculating vertical electron affinities at the B3LYP/6-311+G(2d)//B3LYP/6-31+G(d) level of theory, using the geometries obtained for the non-solvated molecules. All calculations were done with the Gaussian 03 package of programs [42].

### 2.3. Quinone synthesis

The syntheses of 2-methyl-3-methylamino-1,4-naphthoquinone **2**, 2-amino-3-methyl-1,4-naphthoquinone **3**, 2-ethyl-3-methyl-1,4-naphthoquinone **5**, 2,3-dimethyl-1,4-naphthoquinone **6** and 2-methyl-3-nitro-1,4-naphthoquinone **8** have been described previously [21, 22]. 2-Bromo-3-methyl-1,4-naphthoquinone **7** [43] and 6,7-dimethoxy-1,4-naphthoquinone **13** [44] were synthesized following literature procedures.

The synthesis of 2-hexyl-3-methyl-1,4-naphthoquinone **4** was identical to that of 2-ethyl-3-methyl-1,4-naphthoquinone **5** [22], starting from commercially available vitamin K<sub>3</sub>. The hexyl residue was introduced by a radical Hunsdiecker decarboxylation of heptanoic acid using silver nitrate and peroxydisulfate in an acetonitrile/water mixture. <sup>1</sup>H-NMR (250.13 MHz, CDCl<sub>3</sub>): δ[ppm] = 8.12–8.08 (dd, <sup>2</sup>J = 10.0 Hz, <sup>3</sup>J = 2.5 Hz, 2H, aromatic protons), 7.73–7.69 (dd, <sup>2</sup>J = 10.0 Hz, <sup>3</sup>J = 2.5 Hz, 2H, aromatic protons), 2.66 (t, <sup>2</sup>J = 7.5 Hz, 2H, CH<sub>2</sub>CH<sub>2</sub>), 2.22 (s, 3H, CH<sub>3</sub>), 1.27–1.50 (m, 8H, 4×CH<sub>2</sub>) 0.88 (t, <sup>2</sup>J = 7.5 Hz, 3H, CH<sub>2</sub>CH<sub>3</sub>). <sup>13</sup>C-NMR (62.9 MHz, CDCl<sub>3</sub>): δ[ppm] = 185.4; 184.7 (C = O), 147.6; 143.1; 132.2; 132.1 (C), 133.3; 133.2; 126.2; 126.1 (CH), 31.6; 29.6; 28.7; 27.12; 22.5 (CH<sub>2</sub>), 14.0; 12.6 (CH<sub>3</sub>). Anal.Calcld. for C<sub>17</sub>H<sub>20</sub>O<sub>2</sub>: C 79.65, H 7.86; Found: C 79.57, H 7.86.

## 2.4. Electrochemistry

Cyclic voltammetry experiments were measured using a conventional three-electrode cell in dimethoxyethane with tetrabutylammoniumperchlorate as supporting electrolyte on platinum working and counter electrodes. The quinones were used as solutions at concentrations of 1 mM. The potential is given vs. Ag/AgCl reference electrode, with a voltage sweep rate of 50 mV s<sup>-1</sup> or 20 mV s<sup>-1</sup>. 1,2-dimethoxyethane (DME) was purchased from Fluka, puriss; dried over molecular sieves (H<sub>2</sub>O < 0.005%). The solutions of the quinones were deoxygenated with dry nitrogen prior use and maintained under inert nitrogen condition during each experimental run. The reversibility of the cyclic voltammograms was evaluated (Supplementary material S3). The one-electron peaks remain stable after different runs and different scan rates. All electrochemical experiments were performed at 25°C. The midpoint potentials remained almost constant under variation of the concentration, shown i.e. for quinones **2** and **6** respectively when the 1 mM solutions were diluted from 1 mM to 0.5 mM solution and to 0.25 mM (see Supplementary material S2–S3). Differential pulse voltammetry experiments were performed on a CHI620 electrochemical analyzer. A standard three-electrode system with Pt platelets as working and counter electrodes was used. As a reference, a Ag/NBu<sub>4</sub>PF<sub>6</sub>/MeCN electrode with a Haber–Luggin capillary was used.

## 2.5. X-ray crystal structure analysis

Single crystals of the naphthoquinones **2**, **3**, **4**, **5**, **7**, **9** and **13** suitable for X-ray crystal structure analysis were obtained from dichloromethane solution. The structures of 2-methyl-3-methylamino-1,4-naphthoquinone **3** and 2-ethyl-3-methyl-1,4-naphthoquinone **5** contain two crystallographically independent molecules. Both molecules possess a very similar conformation. In all naphthoquinones the benzene ring is planar while the benzoquinone ring shows a small deviation from planarity in some structures. The resulting crystal structures can be compared to those of **1** [45] and **6** [46]. Crystallographic data of compounds **2**, **3**, **4**, **5**, **7**, **9** and **13** have been deposited with Cambridge Crystallographic Data Center. Copies of the data can be obtained free of charge via [www.ccdc.cam.ac.uk/conts/retrieving.html](http://www.ccdc.cam.ac.uk/conts/retrieving.html).

CCDC-640771; Nr. **2** dark brown block; chemical formula C<sub>12</sub>H<sub>11</sub>NO<sub>2</sub>; formula weight (*M*) 201.22; crystal system Monoclinic; Unit-cell *a* = 17.602(4) Å, *b* = 9.6348(17) Å, *c* = 13.187(3) Å,  $\alpha$  = 90°,  $\beta$  = 120.081(14)°,  $\gamma$  = 90°; space group C 2/c; *Z* = 8;  $\mu$  = 0.095 mm<sup>-1</sup>; number of measured reflections 16186; number of independent reflections 3038; final *R*: *R*<sub>1</sub> = 0.044 *wR*<sub>2</sub> = 0.119. 2-methyl-3-methylamino-1,4-naphthoquinone **2** forms dimers connected by rather weak intermolecular NH...O hydrogen bonds. The NH group shows an additional hydrogen bond as a weak intramolecular NH...O contact.  $\theta$  H1–N–C1–C2 = 2 (1)°. O...H 2.09(2) [Å].

CCDC-640772; Nr. **3** red rod; chemical formula C<sub>11</sub>H<sub>9</sub>NO<sub>2</sub>·0.5H<sub>2</sub>O; formula weight (*M*) 196.20; crystal system Monoclinic; Unit-cell *a* = 17.048(9) Å, *b* = 3.831(2) Å, *c* = 27.879(16) Å,  $\alpha$  = 90°,  $\beta$  = 97.97 (3)°,  $\gamma$  = 90°; space group P 2<sub>1</sub>/n; *Z* = 8;  $\mu$  = 0.104 mm<sup>-1</sup>; number of measured reflections 19,470; number of independent reflections 4063; final *R*: *R*<sub>1</sub> = 0.122 *wR*<sub>2</sub> = 0.201. Each NH<sub>2</sub> group is involved in a weak intramolecular NH...O hydrogen bond and an intermolecular NH...O Hydrogen bond.  $\theta$  H1B–N1–C1–C2 = 9 (7)°. H2B–N2–C12–C13 = 1(4)° H2B–O5 2.35(5) H1B–O2 2.24(9) [Å].

CCDC-640773; Nr. **4** pale yellow needle; chemical formula C<sub>17</sub>H<sub>20</sub>O<sub>2</sub>; formula weight (*M*) 256.33; crystal system Monoclinic; Unit-cell *a* = 7.684(3) Å, *b* = 4.765(2) Å, *c* = 19.333(6) Å,  $\alpha$  = 90°,  $\beta$  = 93.043 (17)°,  $\gamma$  = 90°; space group P 2<sub>1</sub>; *Z* = 2;  $\mu$  = 0.077 mm<sup>-1</sup>; number of measured reflections 8184; number of independent reflections 1732; final *R*: *R*<sub>1</sub> = 0.087 *wR*<sub>2</sub> = 0.161. The hexane group has an all-*trans* conformation. The C11–C12 bond has an orientation almost perpendicular to the naphthoquinone plane.  $\theta$  C2–C1–C11–C12 84.4 (6)°.

CCDC-640774; Nr. **5** yellow block; chemical formula C<sub>13</sub>H<sub>12</sub>O<sub>2</sub>; formula weight (*M*) 200.23; crystal system Triclinic; Unit-cell *a* = 7.9978(10) Å, *b* = 10.0437(15) Å, *c* = 13.2982(14) Å,  $\alpha$  = 91.623 (7)°,  $\beta$  = 102.423(7)°,  $\gamma$  = 95.861(7)°; space group P  $\bar{1}$ ; *Z* = 4;  $\mu$  = 0.086 mm<sup>-1</sup>; number of measured reflections 17,078; number of independent reflections 5771; final *R*: *R*<sub>1</sub> = 0.056 *wR*<sub>2</sub> = 0.128.  $\theta$  C10–C11–C12–C13 = 91.2 (2)°. C23–C24–C25–C26 89.7 (2)°.

CCDC-640775; Nr. **7** yellow rod; chemical formula C<sub>11</sub>H<sub>7</sub>BrO<sub>2</sub>; formula weight (*M*) 251.08; crystal system Monoclinic; Unit-cell *a* = 7.3187(10) Å, *b* = 8.3629(13) Å, *c* = 14.8943(19) Å,  $\alpha$  = 90°,  $\beta$  = 91.581(11)°,  $\gamma$  = 90°; space group P 2<sub>1</sub>/n; *Z* = 4;  $\mu$  = 4.475 mm<sup>-1</sup>; number of measured reflections 16,110; number of independent reflections 3322; final *R*: *R*<sub>1</sub> = 0.050 *wR*<sub>2</sub> = 0.105. The crystal packing shows an intermolecular CH...Br, CH... $\pi$  (benzene) and  $\pi$  (benzene)... $\pi$  (quinone) interaction.

CCDC-640776; Nr. **9** yellow needle; chemical formula C<sub>11</sub>H<sub>8</sub>O<sub>3</sub>; formula weight (*M*) 188.17; crystal system Monoclinic; Unit-cell *a* = 7.6626(13) Å, *b* = 4.8585(8) Å, *c* = 11.6463(16) Å,  $\alpha$  = 90°,  $\beta$  = 90.186(12)°,  $\gamma$  = 90°; space group P 2<sub>1</sub>; *Z* = 2;  $\mu$  = 0.106 mm<sup>-1</sup>; number of measured reflections 5560; number of independent reflections 1340; final *R*: *R*<sub>1</sub> = 0.048 *wR*<sub>2</sub> = 0.087. The molecules are connected by OH...O hydrogen bonds to zig-zag chains in the *b*-direction. The OH group also is involved in an intramolecular OH...O contact. The molecules form stacks in the *b*-direction. Molecules in the stacks show partial overlapping  $\pi$  systems. The  $\pi$ ... $\pi$ -distances in the stacks are about 3.50 Å.  $\theta$  H1–O1–C1–C2 = 6 (2)°. O...H 2.18(3) [Å].

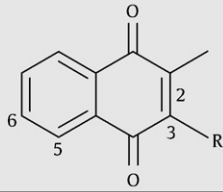
CCDC-640777; Nr. **13** yellow prism; chemical formula C<sub>12</sub>H<sub>10</sub>O<sub>4</sub>; formula weight (*M*) 218.20; crystal system Monoclinic; Unit-cell *a* = 6.8510(16) Å, *b* = 15.553(4) Å, *c* = 4.7944(13) Å,  $\alpha$  = 90°,  $\beta$  = 108.132(12)°,  $\gamma$  = 90°; space group C *m*; *Z* = 2;  $\mu$  = 0.113 mm<sup>-1</sup>; number of measured reflections 3169; number of independent reflections 751; final *R*: *R*<sub>1</sub> = 0.051 *wR*<sub>2</sub> = 0.112.

## 3. Results and discussion

Vitamin K<sub>3</sub> is the redox active core of vitamin K, the aliphatic side chain found at the 3-position in vitamin K is replaced by a hydrogen atom in vitamin K<sub>3</sub>. In this work, we use vitamin K<sub>3</sub> **1** as starting point for an electrochemical study. For this purpose, in addition to the five quinones (**2**, **3**, **8** [21] and **5**, **6** [22]) synthesized previously 2-hexyl-3-methyl-1,4-naphthoquinone **4** and 2-Bromo-3-methyl-1,4-naphthoquinone **7** [43] were prepared and characterized by cyclic voltammetric measurements (Table 1).

**Table 1**

Vitamin K<sub>3</sub> derivatives investigated in this study, their corresponding midpoint potential *E*<sub>1/2</sub> and the difference *E*<sub>pa</sub> – *E*<sub>pc</sub>.

		<i>R</i>	<i>E</i> <sub>pa</sub> – <i>E</i> <sub>pc</sub> [V]	<i>E</i> <sub>1/2</sub> [V]
<b>1</b>	H (Vitamin K <sub>3</sub> )	H	0.19	–0.635
<b>2</b>	NHMe	NHMe	0.18	–0.840
<b>3</b>	NH <sub>2</sub>	NH <sub>2</sub>	0.18	–0.810
<b>4</b>	(CH <sub>2</sub> ) <sub>5</sub> CH <sub>3</sub>	(CH <sub>2</sub> ) <sub>5</sub> CH <sub>3</sub>	0.22	–0.770
<b>5</b>	CH <sub>2</sub> CH <sub>3</sub>	CH <sub>2</sub> CH <sub>3</sub>	0.20	–0.770
<b>6</b>	CH <sub>3</sub>	CH <sub>3</sub>	0.19	–0.765
<b>7</b>	Br	Br	0.16	–0.490
<b>8</b>	NO <sub>2</sub>	NO <sub>2</sub>	0.19	–0.255
<b>9</b>	OH	OH	– <sup>a</sup>	–

<sup>a</sup> phthiol **9** exhibits a single irreversible 2/3-electron peak [48] with *E*<sub>pc</sub> = –0.62 V.



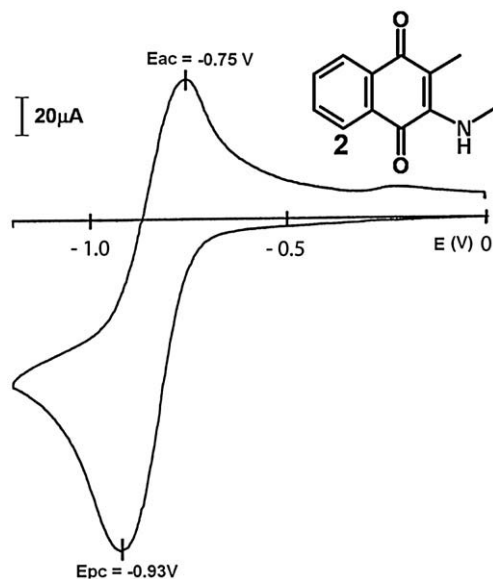


**Fig. 1.** Cyclic voltammogram of **2** (1 mM) in 1,2-dimethoxyethane (DME) with tetrabutylammoniumperchlorate as supporting electrolyte ( $10^{-1}$  mM) on platinum working and counter electrodes. The potential is given vs. Ag/AgCl reference electrode with a voltage sweep rate of  $50 \text{ mV s}^{-1}$ .  $E_{pc} = -0.93 \text{ V}$ ,  $E_{pa} = -0.75 \text{ V}$ ,  $E_{pa} - E_{pc} = 0.18 \text{ V}$  and  $E_{1/2} = (E_{pa} + E_{pc}) / 2 = -0.84 \text{ V}$ .

In this study we use the thermodynamically relevant midpoint potential  $E_{1/2}$  (Fig. 1). The neutral naphthoquinone structures were subjected to X-ray crystal structure analyses.

Single crystals of the vitamin K<sub>3</sub> analogues **2**, **3** [47], **4**, **5**, **7** and **9** [47] were obtained from dichloromethane solution, their crystal properties which are summarized and discussed in the **Materials and methods** and were used as starting point for our DFT calculation.

To the set of compounds (table 1) was chosen according to the following considerations. Substituents such as amino or methylamino should lower the midpoint potential  $E_{1/2}$ , when replacing the 3-hydrogen atom in vitamin K<sub>3</sub> (**2** and **3**). By contrast substituents such as bromine **7** and nitro **8** should increase the  $E_{1/2}$ . In the case of the alkyl-substituted vitamin K<sub>3</sub> analogues (**4**, **5**, and **6**), the midpoint potential  $E_{1/2}$  should slightly decrease due to the inductive effect exerted by the methylene groups. The midpoint potential  $E_{1/2}$  for the quasi-reversible first reduction step of the quinones to the corresponding semiquinone radical anions (cathodic peak potentials  $E_{pc}$ ) and the first oxidation step of these species to the quinones (anodic peak potentials  $E_{ap}$ ) was measured by cyclic voltammetry in 1,2-dimethoxyethane (DME) as an aprotic polar solvent (Fig. 1).

With the exception of **9** (Supplementary material S1), for all naphthoquinone a quasi-reversible one-electron peak ( $E_{pa} - E_{pc} > 59 \text{ mV}$ ) was observed and the cathodic peak potential did not change with varying scan rate (for **2**  $E_{pc} = -0.93 \text{ V}$  vs. Ag/AgCl reference electrode, with a voltage sweep rate of  $50 \text{ mV s}^{-1}$ ). In general, the measured thermodynamic midpoint potentials show the expected trends for different substituents, high values for substituents such as  $R = \text{NH}_2$  and lower values for  $R = \text{NO}_2$ , for instance. The relative redox potentials for different quinones as isolated compounds are compatible to those for the respective protein bound-forms obtained by *in situ* redox potential measurements [21]. For comparison purposes, more sensitive differential pulse voltammetry have been applied. The results, however, indicate that the potential difference of different quinones is nearly identical regardless of the particular method applied (Supplementary material S4). Vertical and adiabatic electron affinities ( $E_A$ ) of a series of 2-methylnaphthoquinones with different substituents at the carbon atom C-3 were calculated using density functional methods. Density functional theory turns out to be

an accurate method [48,49] to approach the single electrochemical reduction and its relation to enzyme–cofactor interactions by allowing the incorporation of non-covalent interactions, which are present in protein–cofactor complexes in our calculations. The calculated values were compared with the experimental midpoint potentials  $E_{1/2}$  determined by cyclic voltammetry [50]. As summarized in Fig. 2, the theoretical  $E_A$  values are linearly correlated with that of the experimental  $E_{1/2}$  values. A fair correlation between theoretical and experimental data could be established for both vertical as well as for adiabatic electron affinities.

Due to the relaxation of the geometry of the radical anion, the adiabatic electron affinities are generally more negative. Solvent effects have been introduced on the basis of the polarisable continuum model (PCM) using vertical electron affinities for the solvent THF as a model for DME. The use of THF results in an additional lowering of the computed  $E_A$ , due to a more favourable interaction of the radical anion with the solvent. However this correlation does not improve the quality of the correlation significantly. The correlations shown in Fig. 2 allow a prediction of the reduction potentials for naphthoquinones with new substitution patterns on the basis of computed electron affinities. In qualitative agreement with all experimental data, the theoretical electron affinities show a clear dependence on the type of the substituent for the 2-methylnaphthoquinone series substituted at C-3 (Table 2, column A).

While electron-donating substituents such as  $\text{NH}_2$  result in low electron affinities ( $E_A = -1.441 \text{ eV}$ ), electron-withdrawing substituents such as  $\text{NO}_2$  result in the highest electron affinities ( $E_A = -2.286 \text{ eV}$ ). Alkyl-, hydroxyl-, mercapto- and halogen substituents give rise to intermediate sized values that range from  $-1.634 \text{ eV}$  ( $R = \text{CH}_3$ ) to  $-1.962 \text{ eV}$  ( $R = \text{Br}$ ). The hydroxyl substituted naphthoquinone has a slightly smaller electron affinity than its mercapto analogue. The replacement of the hydroxyl- or mercapto-groups with methoxy- or thioether-groups has significant influences on the calculated electron affinities ( $E_A(\text{OH}) = -1.750 \text{ eV}$ ,  $E_A(\text{OMe}) = -1.617 \text{ eV}$ ;  $E_A(\text{SH}) = -1.851 \text{ eV}$ ,  $E_A(\text{SMe}) = -1.752 \text{ eV}$ ). The stronger electron-donating abilities of alkoxy- and thioether-groups result in significantly lower electron affinities. For quinones with halogen substituents, a significant trend is also predicted. Substitution with a fluorine atom, which has not only an inductive-withdrawing effect but also the largest  $\pi$  donating effect compared to its heavier homologues leads to the smallest predicted  $E_A$  values among the halogen substituted quinones ( $E_A(\text{F}) = -1.853 \text{ eV}$ ,  $E_A(\text{Br}) = -1.962 \text{ eV}$ ). This trend indicates that the  $\pi$ -donating effect is predominant over the  $\sigma$ -

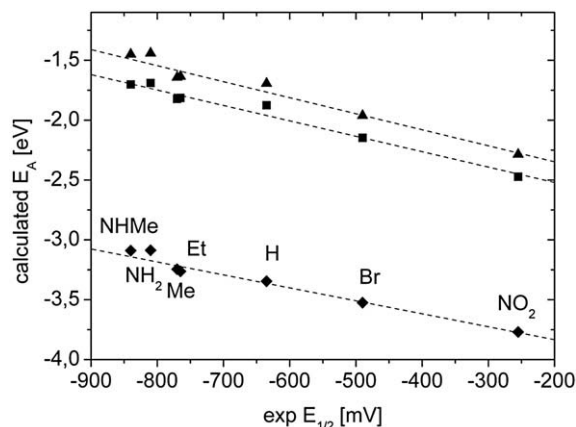


**Fig. 2.** Correlation of calculated electron affinities  $E_A^{\text{calc}}$  with experimental midpoint potentials  $E_{1/2}^{\text{exp}}$ . Vertical electron affinities  $\blacktriangle$ :  $E_A^{\text{calc}} = (-2.62 \pm 0.07) - (0.00134 \pm 0.001) E_{1/2}^{\text{exp}}$ ,  $R = 0.99$ . Adiabatic electron affinities  $\blacklozenge$ :  $E_A^{\text{calc}} = (-2.78 \pm 0.06) - (0.00129 \pm 0.0001) E_{1/2}^{\text{exp}}$ ,  $R = 0.99$ . Vertical electron affinities using the PCM model to account for solvent effects, THF  $\blacksquare$ :  $E_A^{\text{calc}} = (-4.05 \pm 0.05) - (0.00118 \pm 0.00007) E_{1/2}^{\text{exp}}$ ,  $R = 0.99$ .

**Table 2**  
Calculated vertical electron affinities of quinones with different substitution patterns.

		Calculated $E_A$ [eV]		
		A <sup>a</sup>	B <sup>c</sup>	C <sup>b</sup>
R				
Compound				
NH <sub>2</sub>	in-plane	–1.441	–1.423	–1.494
	perpendicular	–1.557		
NHMe		–1.449	–1.348	–1.512
NMe <sub>2</sub>		–1.465	–1.351	–1.384
OMe		–1.617	–1.473	–1.510
CH <sub>3</sub>		–1.634	–1.538	–1.540
CH <sub>2</sub> CH <sub>3</sub>		–1.642	–1.594	–1.587
(CH <sub>2</sub> ) <sub>2</sub> CH <sub>3</sub>		–1.635	– <sup>d</sup>	– <sup>d</sup>
(CH <sub>2</sub> ) <sub>3</sub> CH <sub>3</sub>		–1.636	– <sup>d</sup>	– <sup>d</sup>
(CH <sub>2</sub> ) <sub>5</sub> CH <sub>3</sub>		–1.639	– <sup>d</sup>	– <sup>d</sup>
H		–1.693		
OH		–1.750	–1.561	–1.507
SMe		–1.752	– <sup>d</sup>	– <sup>d</sup>
SH		–1.851	–1.724	–1.826
F		–1.853	–1.780	–1.738
Cl		–1.932	–1.856	–1.768
Br		–1.962	–1.877	–1.792
CF <sub>3</sub>		–2.108	–2.019	–1.894
NO <sub>2</sub>	perpendicular	–2.286	–2.350	–2.093
	in-plane	–2.392		

<sup>a</sup> 2-Me, 3-R.

<sup>b</sup> 2-Me, 3-Me, 5-R.

<sup>c</sup> 2-Me, 3-Me, 6-R.

<sup>d</sup> Not determined.

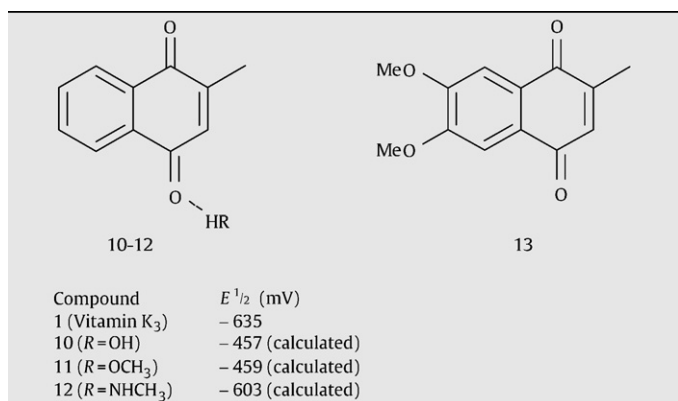
withdrawing effect. For the alkyl-substituted vitamin K<sub>3</sub> derivatives **4–6**, the elongation of the side chain has a negligible effect on the electrochemical behaviour (the decyl substituted derivative has nearly the same cathodic peak potential as vitamin K<sub>2</sub>; data not shown). In agreement with the experiment, almost constant electron affinities have been calculated for different alkyl groups at C-3 ( $E_A$  (CH<sub>3</sub>) = –1.634 to  $E_A$  (CH<sub>2</sub>)<sub>5</sub>CH<sub>3</sub> = –1.639 eV). This finding indicated that the exhibited binding specificity of the quinone hydrophobic tail in quinone converting enzymes [51,52] is not due to the electrochemical nature of the alkyl substitution. Neither the electrochemical properties, nor the enhancement of the hydrophobicity is the crucial driving force for binding, however, a specific molecular recognition event between the methyl branch and the  $\pi$ -electron system in the isoprene unit [9] occurs. For example one ligand bearing an identical side chain can bind via two different conformations to two different enzymes [53], the two conformations differ in the position of the side chain resides relative to the ring. Our crystal structures of the vitamin K<sub>3</sub> derivatives **4** and **5** shows, in solid state, the side chain perpendicular to the ring. This conformation also was found for the UQ-10 anion radical in the reaction centre (Q<sub>A</sub> site) [54]. Strongly inductive-withdrawing substituents such as R = CF<sub>3</sub> give rise to high computed electron affinities. For R = NO<sub>2</sub>, which in principle has a strong electron withdrawing effect operative by both inductive as well as resonance effects the electron affinity is shifted to even more negative values. Calculations show, however, that in the optimized molecular structure of 2-methyl-3-nitronaphthoquinone **8**, the nitro group is orientated almost perpendicular ( $\theta = 90^\circ$ ) to the naphthoquinone backbone. This indicates that the  $\sigma$ -withdrawing effect is solely responsible for the very high computed  $E_A$  of 2-methyl-3-nitronaphthoquinone **8**. For substituents such as NH<sub>2</sub> and NO<sub>2</sub>, the calculated electron affinities are strongly dependent on the conformation of the substituent. In the energetically most favoured conformation of 2-amino-3-methylnaphthoquinone which has the NH<sub>2</sub> group in an in-plane conformation

with the quinone moiety the electron affinity is significantly lower ( $E_A = -1.441$  eV) than in the perpendicular conformation ( $E_A = -1.557$  eV). An analogous behaviour is calculated for 2-methyl-3-nitronaphthoquinone **8** (Table 2 and S5 in Supplementary material). The orientation of the quinone within the binding pocket of a protein is an important issue. For example, in the photosynthetic reaction centre light-induced conformational changes were used to switch the quinone in the Q<sub>B</sub> site through a 180° propeller twist around the side chain from one position where the electron transfer from Q<sub>A</sub> is inhibited to an alternative position where it is not [6]. Similar allosteric regulation of the electron-transfer reaction can be achieved by an interplay of substituent conformation and electron affinity in quinone reductases [55]. This modulation constitutes an important factor in the fine tuning of the electrochemistry of the quinone cofactor within the binding pocket of the protein. As shown above, it has been found that within 2,3-dimethylnaphthoquinone series B and C with different substituents at C5 and C6, electron-withdrawing substituents give higher electron affinities than electron-donating substituents. It must be emphasized that no simple trends are observable when isomeric molecules (series A, B and C) are compared. The electron affinities of the compounds within series B and C (Table 2) for a given substituent R are more positive compared to the 2-methyl-1,4-naphthoquinone series substituted at C-3, which is due to the electron-donating effect of the additional methyl group. Quinones with the substituents R = NH<sub>2</sub>, NHMe, NO<sub>2</sub> do, however, not follow this trend. In the present study, the quinone with the lowest electron affinity is 5-amino-2,3-dimethyl-1,4-naphthoquinone.

For R = NMe<sub>2</sub> and R = NHMe the calculated electron affinities (R = NMe<sub>2</sub>  $E_A = -1.351$  eV, R = NHMe  $E_A = -1.348$  eV) are about 0.1 eV higher than calculated for 3-dimethylamino-2-methylnaphthoquinone ( $E_A = -1.465$  eV) and 2-methyl-3-methylamino-1,4-naphthoquinone **2** ( $E_A = -1.449$  eV), respectively. The highest  $E_A$  values are predicted for R = NO<sub>2</sub>, in particular for 5-nitro-2,3-dimethyl-1,4-naphthoquinone ( $E_A = -2.350$  eV). In some cases, the computed  $E_A$  values of the naphthoquinones A and B are quite similar for a given substituent R (R = F, Cl, Br, CF<sub>3</sub>, NO<sub>2</sub>), while values predicted for compounds from series C deviate significantly. This observation is a characteristic feature of substituents with the highest calculated electron affinities. In contrast, for most of the stronger electron-donating groups, e.g. R = NMe<sub>2</sub>, OMe, CH<sub>3</sub>, CH<sub>2</sub>CH<sub>3</sub>, OH the results for B and C are comparable. The electron affinities of quinones A, B and C with R = NHMe, NH<sub>2</sub>, SH do not comply with these simple rules. The electron affinity of naphthoquinones can be adjusted by two factors. Firstly, a variation of the substituents R from R = NH<sub>2</sub> to R = NO<sub>2</sub> alters the  $E_A$  values by approximately 0.8 eV. Secondly, as exemplified for 2-amino-3-methyl-1,4-naphthoquinone **3** and 2-methyl-3-nitro-1,4-naphthoquinone **8**, conformational changes can adjust the  $E_A$  value by approximately 0.1 eV (Table 2). Upon binding, significant conformational changes can be induced in the quinone, which results in different electron affinities. Applying the correlation of Fig. 2, a difference in the  $E_A$  of 0.1 eV corresponds to a predicted difference in the reduction potential of 75 mV. This value can be compared to an estimated shift of approximately 100 mV, which can be induced by the interaction between the cofactor and its protein environment [24,56]. Besides conformational changes induced upon binding to a protein, other factors can affect the electron affinity of naphthoquinones, for example the formation of hydrogen bonds between quinones and the biological targets. It has been shown that in synthetic guest–host systems the electrochemical property of a redox active guest is modulated by the host using hydrogen bond formation [57]. For the related cofactor flavin, one finds the same operative non-covalent interactions upon the binding to the enzyme pocket and the environment [58]. With the exception of some examples of covalently bounded quinone cofactors [59], most quinone cofactors are buried in the hydrophobic protein interior and are held by an accumulation of attractive non-covalent interactions, in particular hydrogen bonding

has been shown to play a dominate role. The crystal structure of the quinone–enzyme complex provides detailed information about this dominate non-covalent interaction. The precise adjustment of the quinone into the enzyme pocket and thereby the formation of the non-covalent interaction is crucial for enzyme activity [60].

We investigate the role of hydrogen bonding interactions by using smaller model systems, i.e. adducts of small molecules like water, methanol or methylamine with vitamin K<sub>3</sub>. In these model systems the quinone–water complex plays an outstanding role. In the bovine mitochondrial [61] and yeast [8] cytochrome *bc*<sub>1</sub> complex crystal structures, one or two water molecules are localized at the quinone reduction (Q<sub>i</sub>) site and are involved in the mechanism of quinone reduction and protonation. An  $E_{1/2}$  value can be predicted by applying the correlation in Fig. 2 to the calculated adiabatic electron affinities of **10**, **11** and **12**. The formation of the hydrogen-bonded complexes **10–12** leads to a significant increase of the electron affinities, due to a decrease of electron density at the keto group. In the case of the methanol-vitamin K<sub>3</sub> complex **11**, the electron affinity has the largest negative value ( $E_A$  adiabatic = −2.188 eV) with a predicted midpoint potential  $E_{1/2}$  predicted = −459 mV, while for **12** the smallest change compared to free Vitamin K<sub>3</sub> is predicted ( $E_A$  adiabatic = −2.002 eV,  $E_{1/2}$  predicted = −603 mV). The electron affinity of the water adduct **10** is very close to that of **11** ( $E_A$  adiabatic = −2.167 eV,  $E_{1/2}$  predicted = −457 mV).



Based on the computed electron affinities, biological activities of quinones cannot only be rationalized but also predicted. For example quinones with low electron affinities such as 2-amino-3-methyl-1,4-naphthoquinone **3** or 2-methyl-3-methylamino-1,4-naphthoquinone **2** are converted by QFR (quinol: fumarate reductase) as substrates [21]. This finding makes it possible to predict substituents and substitution patterns of quinones with desired biological activity.

On the basis of a comparison of electron affinities it is also possible to predict the reactivity of quinone radical anions towards molecular oxygen, a reaction which was shown to be important for redox cycling and in and oxidative stress[5]. Quinones with higher  $E_A$  values ( $R=NH_2$ ,  $E_A = -1.441$  eV to  $R=OH$ ,  $E_A = -1.750$  eV, series A) than molecular oxygen ( $E_A = -1.753$  eV) should shift the equilibrium in Eq. (1) to the left, while quinones having lower  $E_A$  values ( $R=SH$ ,  $E_A = -1.851$  eV to  $R=NO_2$ ,  $E_A = -2.286$  eV, series A) shift the equilibrium to the right:



A comparison of experimental reduction potential ( $E_{1/2} = -652$  mV) and predicted reduction potential ( $E_{1/2}$ , predicted = −696 mV) of 6,7-dimethoxy-1,4-naphthoquinone **13** on the basis of

the established correlation using vertical electron affinities (Fig. 2) suggests that this correlation is not confined to quinones with the considered substitution pattern but is also valid for naphthoquinones in general.

### Note added in proof

Our predicted and calculated shift in electron affinity induced by hydrogen bonding in the vitamin K<sub>3</sub> - water complex compared to vitamin K<sub>3</sub> has recently been determined experimentally (Y. Hui, J. Am. Chem. Soc. (2009) 131, 1523–1524).

### Acknowledgments

The authors thank Prof. Thomas Prisner, Prof. Gunther Wittstock and Nadine Jacobs for access to the cyclic and differential pulse voltammetry equipment. The Center for Biomolecular Magnetic Resonance (BMRZ) is supported by the state Hesse. This work was supported by the Deutsche Forschungsgemeinschaft through SFB 472 “Molecular Bioenergetics” and through “Cluster of Excellence: Macromolecular Complexes” and the Fonds der Chemischen Industrie.

### Appendix A. Supplementary data

Supplementary data associated with this article can be found, in the online version, at doi:10.1016/j.bbabbio.2009.02.013.

### References

- [1] S. Patai (Ed.), The Chemistry of Quinoid Compounds, New-York, Wiley and Sons, 1974.
- [2] A.P. Kourounakis, A.N. Assimopoulou, V.P. Papageorgiou, A. Gavalas, P.N. Kourounakis, Alkannin and shikonin: effect on free radical processes and on inflammation – a preliminary pharmacological investigation, Arch. Pharm. 6 (2002) 262–266.
- [3] A. Fujiwara, T. Mori, A. Iida, S. Ueda, Y. Hano, T. Nomura, H. Tokuda, H. Nishino, Antitumor-promoting naphthoquinones from *Catalpa ovata*, J. Nat. Prod. 61 (1998) 629–632.
- [4] a) L. Trumpower, Functions of Quinones in Energy conserving Systems. Academic Press, New York, 1982. b) F.L. Crane, Comments on the discovery of coenzyme Q: a commentary on ‘Isolation of a Quinone from Beef Heart Mitochondria’, Biochim Biophys. Acta 1000 (1989) 358–361.
- [5] a) H. R. Nasiri, M. Bolte, H. Schwalbe, Electrochemical and crystal structural analysis of alpha- and dehydro-alpha-lapachones, Natural Prod. Res. 14 (2008) 1231–1234. b) A. Brisch-Wittmeyer, A.S.S. Sido, P. Guilini, L. Désaubry, Concise synthesis and voltammetric studies of dielsquinone, a cytotoxic azaanthraquinone, Bioorg. Med. Chem. Lett. 15 (2005) 3609–3610 c) S.W. Ham, J. Choe, M. Wang, V. Peyregne and B. Carr, Fluorinated quinoid inhibitor: possible “pure” arylator predicted by the simple theoretical calculation, Bioorg. Med. Chem. Lett. 14 (2004) 4103–4105.
- [6] a) M. H. B. Stowell, T. M. McPhillips, D. C. Rees, S. M. Soltis, E. Abresch, G. Feher, Light-induced structural changes in photosynthetic reaction center: implications for mechanism of electron-proton transfer, Science 276 (1997) 812–816. b) C. R. D. Lancaster, H. Michel, The coupling of light-induced electron transfer and proton uptake as derived from crystal structures of reaction centers from *Rhodospseudomonas viridis* modified at the binding site of the secondary quinone, Q<sub>B</sub>, Structure 5 (1997) 1339–1359.
- [7] a) V. Yankovskaya, R. Horsefield, S. Törnroth, C. Luna-chavez, H. Miyoshi, C. Léger, B. Byrne, G. Cecchini, S. Iwata, Architecture of succinate dehydrogenase and reactive oxygen species generation, Science 299 (2003) 700–704. b) R. Horsefield, V. Yankovskaya, G. Sexton, W. Whittingham, K. Shiomi, S. Omura, B. Byrne, G. Cecchini, S. Iwata, Structural and computational analysis of the quinone-binding site of complex II (succinate-ubiquinone oxidoreductase): a mechanism of electron transfer and proton conduction during ubiquinone reduction, J. Biol. Chem. 281 (2006) 7309–7316.
- [8] C. Hunte, J. Koepke, C. Lange, Tanja Ro manith, H. Michel, Structure at 2.3 Å resolution of the cytochrome *bc*<sub>1</sub> complex from the yeast *Saccharomyces cerevisiae* co-crystallized with an antibody Fv fragment, Structure 8 (2000) 669–684.
- [9] K. Sakamoto, H. Miyoshi, M. Ohshima, K. Kuwabara, K. Kano, T. Akagi, T. Mogi, H. Iwamura, Role of the isoprenyl tail of ubiquinone in reaction with respiratory enzymes: studies with bovine heart mitochondrial complex I and *Escherichia coli* bo-type ubiquinol oxidase, Biochemistry 37 (1998) 15106–15113.
- [10] S.P. Mayalarp, R.H.J. Hargreaves, J. Butler, C.C. O’Hare, J.A. Hartley, Cross-linking and sequence specific alkylation of DNA by aziridinylquinones. 1. Quinone methides, J. Med. Chem. 39 (1996) 531–537.
- [11] S.R. Rajski, R.M. Williams, DNA cross-linking agents as antitumor drugs, Chem. Rev. 98 (1998) 2723–2796.



- [12] K.R. Kunz, B.S. Iyengar, R.T. Dorr, D.S. Alberts, W.A. Remers, Structure–activity relationships for mitomycin C and mitomycin A analogues, *J. Med. Chem.* 34 (1991) 2281–2286.
- [13] F. Sun, X. Huo, Y. Zhai, A. Wang, J. Xu, D. Su, M. Bartlam, Z. Rao, Crystal structure of mitochondrial respiratory membrane protein complex II, *Cell* 121 (2005) 1043–1057.
- [14] P. Mitchell, Coupling of phosphorylation to electron and hydrogen transfer by a chemi-osmotic type of mechanism, *Nature* 191 (1961) 144–148.
- [15] B.L. Trumpower, The protonmotive Q cycle. Energy transduction by coupling of proton translocation to electron transfer by the cytochrome *bc*<sub>1</sub> complex, *J. Biol. Chem.* 265 (1990) 11409–11412.
- [16] F. Muller, A.R. Crofts, D.M. Kramer, Multiple Q-cycle bypass reactions at the Q<sub>o</sub> site of the cytochrome *bc*<sub>1</sub> complex, *Biochemistry* 41 (2002) 7074–7866.
- [17] J.L. Cape, M.K. Bowman, D.M. Kramer, Reaction intermediates of quinol oxidation in a photoactivatable system that mimics electron transfer in the cytochrome *bc*<sub>1</sub> complex, *J. Am. Chem. Soc.* 127 (2005) 4208–4215.
- [18] a) P. R. Rich, The quinone chemistry of *bc*<sub>1</sub> complexes, *Biochem. Biophys. Acta* 1658 (2004) 165–171, b) T. A. Link, The role of the 'Rieske' iron sulfur protein in the hydroquinone oxidation (Q<sub>o</sub>) site of the cytochrome *bc*<sub>1</sub> complex. The 'proton-gated affinity change' mechanism, *FEBS Lett.* 412 (1997) 257–264.
- [19] A. Osyczka, C.C. Moser, F. Daldal, P.L. Dutton, Reversible redox energy coupling in electron transfer chains, *Nature* 427 (2004) 607–612.
- [20] M. Quan, D. Sanchez, M.F. Wasylkiw, D.K. Smith, Voltammetry of quinones in unbuffered aqueous solution: reassessing the roles of proton transfer and hydrogen bonding in the aqueous electrochemistry of quinones, *J. Am. Chem. Soc.* 129 (2007) 12847–12856.
- [21] M.G. Madej, H.R. Nasiri, N.S. Hilgendorff, H. Schwalbe, C.R.D. Lancaster, Evidence for transmembrane proton transfer in a dihaem-containing membrane protein complex, *EMBO J.* 25 (2006) 4963–4970.
- [22] M.G. Madej, H.R. Nasiri, N.S. Hilgendorff, H. Schwalbe, G. Uden, C.R.D. Lancaster, Experimental evidence for proton motive force-dependent catalysis by the dihaem-containing succinate:menaquinone oxidoreductase from the Gram-positive bacterium *Bacillus licheniformis*, *Biochemistry* 45 (2006) 15049–15055.
- [23] F. C. de Abreu, P.A.L. Ferraz, M.O.F. Goulart, Some applications of electrochemistry in biomedical chemistry. Emphasis on the correlation of electrochemical and bioactive properties, *J. Braz. Chem. Soc.* 13 (2002) 19–35.
- [24] E. Takahashi, T.A. Wells, C.A. Wright, Protein control of the redox potential of the primary quinone acceptor in reaction centers from *Rhodospirillum rubrum*, *Biochemistry* 40 (2001) 1020–1028.
- [25] T.A. Wells, E. Takahashi, C.A. Wright, Primary quinone (QA) binding site of bacterial photosynthetic reaction centers: mutations at residue M265 probed by FTIR spectroscopy, *Biochemistry* 42 (2003) 4064–4074.
- [26] a) D.L. Breen, Coenzyme Q: a molecular orbital study, *J. Theor. Biol.* 53 (1975) 101–113, b) H.H. Robinson, S. D. Kahn, Interplay of substituent conformation and electron affinity in quinone models of quinone reductases, *J. Am. Chem. Soc.* 112 (1990) 4728–4731, c) R. A. Wheeler, A method for computing one-electron reduction potentials and its application to *p*-benzoquinone in water at 300 K, *J. Am. Chem. Soc.* 116 1994 11048–11051.
- [27] a) M. Nonella, A quantum chemical investigation of structures, vibrational spectra and electron affinities of the radicals of quinone model compounds, *Photosynthesis Research* 55 (1998) 253–259, b) U. Zachariae, C. R. D. Lancaster, Proton uptake associated with the reduction of the primary quinone Q(A) influences the binding site of the secondary quinone Q(B) in *Rhodospseudomonas viridis* photosynthetic reaction centers, *Biochim. Biophys. Acta* 1505 (2001) 280–290.
- [28] M. Nonella, A density functional investigation of model molecules for ubisemiquinone radical anions, *J. Phys. Chem. B* 102 (1998) 4217–4225.
- [29] M. Schmidt am Busch, E.W. Knapp, One-electron reduction potential for oxygen- and sulfur-centered organic radicals in protic and aprotic solvents E. J. Am. Chem. Soc. 127 (2005) 15730–15737.
- [30] A.K. Grafton, R.A. Wheeler, A comparison of the properties of various fused-ring quinones and their radical anions using Hartree–Fock and Hybrid Hartree–Fock/density functional methods, *J. Phys. Chem. A* 101 (1997) 7154–7166.
- [31] Y. Pan, Y. Fu, S. Liu, H. Yu, Y. Gao, Q. Guo, S. Yu, Studies on photoinduced H-atom and electron transfer reactions of *o*-naphthoquinones by laser flash photolysis, *J. Phys. Chem. A* 110 (2006) 7316–7322.
- [32] S. Kacprzak, M. Kaupp, F. MacMillan, Protein-cofactor interactions and EPR parameters for the Q(H) quinone binding site of quinol oxidase. A density functional study, *J. Am. Chem. Soc.* 128 (2006) 5659–5671.
- [33] M. Kaupp, C. Remenyi, J. Vaara, O.L. Malkina, V.G. Malkin, Density functional calculations of electronic g-tensors for semiquinone radical anions. The role of hydrogen bonding and substituent effects, *J. Am. Chem. Soc.* 124 (2002) 2709–2722.
- [34] H. Mohapatra, S. Umapathy, Time-resolved resonance Raman spectroscopic studies on the radical anions of methyl-1,4-benzoquinone and 2,6-dimethyl-1,4-benzoquinone, *J. Phys. Chem. A* 106 (2002) 4513–4518.
- [35] S.E. Boesch, A.K. Grafton, R.A. Wheeler, Electron affinities of substituted *p*-benzoquinones from hybrid Hartree–Fock/density-functional calculations, *J. Phys. Chem.* 100 (1996) 10083–10087.
- [36] S. Tsutsui, K. Sakamoto, H. Yoshida, A. Kunai, Cyclic voltammetry and theoretical calculations of silyl-substituted 1,4-benzoquinones, *J. Organomet. Chem.* 690 (2005) 1324–1331.
- [37] A.N. Pankratov, Electron affinities of quinones from quantum chemical data, *Afinidad* 61 (2004) 256–260.
- [38] C. Frontana, A. Vazquez-Mayagoitia, J. Garza, R. Vargas, I. Gonzalez, Substituent effect on a family of quinones in aprotic solvents: an experimental and theoretical approach, *J. Phys. Chem. A* 110 (2006) 9411–9419.
- [39] P. Hammershøj, T.K. Reenberg, M. Pittelkow, C.B. Nielsen, O. Hammerich, J.B. Christensen, Synthesis and properties of 2,3-dialkynyl-1,4-benzoquinones, *Eur. J. Org. Chem.* 12 (2006) 2786–2794.
- [40] A. D. Becke, Density-functional exchange-energy approximation with correct asymptotic behavior, *Phys. Rev. A* 38 (1988) 3098–3100, b) C. Lee, W. Yang, R. G. Parr, Development of the Colle–Salvetti correlation-energy formula into a functional of the electron density, *Phys. Rev. B* 37, (1988) 785–789, c) A. D. Becke, Density-functional thermochemistry. III. The role of exact exchange, *J. Chem. Phys.* 98 (1993) 5648–5652, d) B. G. Johnson, P. M. W. Gill, J. A. Pople, The performance of a family of density functional methods, *J. Chem. Phys.* 98 (1993) 5612–5626.
- [41] a) S. Miertus, E. Scrocco, J. Tomasi, Electrostatic Interaction of a solute with a continuum. a direct utilization of ab initio molecular potentials for the prevision of solvent effects, *Chem. Phys.* 55 (1981) 117–124, b) S. Miertus, J. Tomasi, Approximate evaluations of the electrostatic free energy and internal energy changes in solution processes, *Chem. Phys.* 65 (1982) 239–245, c) M. Cossi, G. Scalmani, N. Rega, V. Barone, New developments in the polarizable continuum model for quantum mechanical and classical calculations on molecules in solution, *J. Chem. Phys.* 117 (2002) 43–54, d) R. Cammi, B. Mennucci, J. Tomasi, Fast evaluation of geometries and properties of excited molecules in solution: a Tamm–Dancoff model with application to 4-dimethylaminobenzonitrile, *J. Phys. Chem. A* 104 (2000) 5631–5637.
- [42] Gaussian 03, Revision C.02, M. J. Frisch et al., Gaussian, Inc., Wallingford CT, 2004.
- [43] R. Adams, T.A. Geissman, B.R. Baker, H.M. Teeter, Structure of Gossypol. XXIV. attempts to prepare desapogossypolone tetramethyl ether, *J. Am. Chem. Soc.* 63 (1941) 528–534.
- [44] J. Reichwagen, H. Hopf, A. Del Guerso, C. Belin, H. Bouas-Laurent, J. Desvergne, Synthesis of 2,3-substituted tetracenes and evaluation of their self-assembling properties in organic solvents, *Org. Lett.* 7 (2005) 971–974.
- [45] H. Nowell, J.P. Attfield, X-Ray and neutron powder diffraction studies of the crystal structure of vitamin K<sub>3</sub>, *New J. Chem.* 28 (2004) 406–411.
- [46] M. Breton-Lacombe, Structures cristallines des dérivés 2 et 3 de la naphthoquinone-1,4, VII. Structure de la diméthyl-2,3-naphthoquinone-1,4, *Acta Crystallogr.* 23 (1967) 1024–1031.
- [47] The crystal structures of compound 3 and 9 were previously determined by P. J. Gaultier and C. Hauw, Structures des dérivés 2 et 3 de la naphthoquinone-1,4, IV. Le phtholol - antagonisme par analogie structurale, *Acta Cryst.* 19 (1965) 919–926 for 9 and Structures cristallines des dérivés 2 et 3 de la naphthoquinone-1,4, VI. Hydrate de méthyl-2-amino-3-naphthoquinone-1,4, 2C11O2NH9.1/2H2O, *Acta Cryst.* 21 (1966) 694–704 for 3. The present determination, however, is considerably more accurate.
- [48] J.C. Rienstra-kiracofe, G.S. Tschumper, H.F. Schaefer III, Atomic and molecular electron affinities: photoelectron experiments and theoretical computations, *Chem. Rev.* 102 (2002) 231–282.
- [49] Y. Fu, L. Liu, H. Yu, Y. Wang, Q. Guo, Quantum-chemical predictions of absolute standard redox potentials of diverse organic molecules and free radicals in acetonitrile, *J. Am. Chem. Soc.* 127 (2005) 7227–7234.
- [50] A. Dhiman, J.D. Becker, O. Minge, H. Schmidbaur, T. Müller, A simple correlation of anodic peak potentials of silylarenes and their vertical ionization energies, *Organometallics* 23 (2004) 1636–1638.
- [51] K. Sakamoto, H. Miyoshi, K. Takegami, T. Mogi, Y. Anraku, H. Iwamura, Probing substrate binding site of the *Escherichia coli* quinol oxidases using synthetic ubiquinol analogues, *J. Biol. Chem.* 271 (1996) 29897–29902.
- [52] M. Ohshima, H. Miyoshi, K. Sakamoto, K. Takegami, J. Iwata, K. Kuwabara, H. Iwamura, T. Yagi, Characterization of the ubiquinone reduction site of mitochondrial complex I using bulky synthetic ubiquinones, *Biochemistry* 37 (1998) 6436–6445.
- [53] C.R. Lancaster, C. Hunte, J. Kelley III, B.L. Trumpower, R. Ditchfield, A comparison of stigmatellin conformations, free and bound to the photosynthetic reaction center and the cytochrome *bc*<sub>1</sub> complex, *J. Mol. Biol.* 368 (2007) 197–208.
- [54] M. Zheng, G.C. Dismukes, The conformation of the isoprenyl chain relative to the semiquinone head in the primary electron acceptor (QA) of higher plant PSII (plastosemiquinone) differs from that in bacterial reaction centers (ubisemiquinone or menasemiquinone) by ca. 90 degrees, *Biochemistry* 35 (1996) 8955–8963.
- [55] H.H. Robinson, S.D. Kahn, Interplay of substituent conformation and electron affinity in quinone models of quinone reductases, *J. Am. Chem. Soc.* 112 (1990) 4728–4731.
- [56] H. Ishikita, E. Knapp, Control of quinone redox potentials in photosystem II: electron transfer and photoprotection, *J. Am. Chem. Soc.* 127 (2005) 14714–14720.
- [57] a) Y. Ge, L. Miller, T. Ouimet, D.K. Smith, Electrochemically controlled hydrogen bonding. *o*-Quinones as simple redox-dependent receptors for arylureas, *J. Org. Chem.* 65 (2000) 8831–8838, b) A.E. Kaifer, The interplay between molecular recognition and redox chemistry, *Acc. Chem. Res.* 32 (1999) 62–71, c) J.H.R. Tucker, S.R. Collinson, Recent developments in the redox-switched binding of organic compounds, *Chem. Soc. Rev.* 31 (2002) 147–156, d) G. Cooke, V.M. Rotello, Methods of modulating hydrogen bonded interactions in synthetic host-guest systems, *Chem. Soc. Rev.* 31 (2002) 275–286.
- [58] a) L.H. Bradley, R.P. Swenson, Role of hydrogen bonding interactions to N(3)H of the flavin mononucleotide cofactor in the modulation of the redox potentials of the Clostridium beijerinckii flavodoxin, *Biochemistry* 40 (2001) 8686–8695, b) K. Yang, R.P. Swenson, Modulation of the redox properties of the flavin cofactor through hydrogen-bonding interactions with the N(5) atom: role of alphaSer254 in the electron-transfer flavoprotein from the methylotrophic bacterium W3A1, *Biochemistry* 46 (2007) 2289–2297, c) A. Niemz, V.M. Rotello, From enzyme to molecular device. exploring the interdependence of redox and molecular recognition, *Acc. Chem. Res.* 32 (1999) 44–52.
- [59] a) S.M. Janes, D. Mu, D. Wemmer, A.J. Smith, S. Kaur, D. Maltby, A.L. Burlingame, J.P. Klinman, A new redox cofactor in eukaryotic enzymes: 6-hydroxydopa at the

- active site of bovine serum amine oxidase, *Science* 248 (1990) 981–987. b) S.X. Wang, M. Mure, K.F. Medzihradszky, A.L. Burlingame, D.E. Brown, D.M. Dooley, A.J. Smith, H.M. Kagan, J.P. Klinman, A crosslinked cofactor in lysyl oxidase: redox function for amino acid side chains, *Science* 273 (1996) 1078–1084. c) W.S. McIntire, D.E. Wemmer, A. Chistoserdov, M.E. Lidstrom, A new cofactor in a prokaryotic enzyme: tryptophan tryptophylquinone as the redox prosthetic group in methylamine dehydrogenase, *Science* 252 (1991) 817–824.
- [60] T. Wenz, P. Hellwig, F. MacMillan, B. Meunier, C. Hunte, Probing the role of E272 in quinol oxidation of mitochondrial complex III, *Biochemistry* 45 (2006) 9042–9052.
- [61] X. Gao, X. Wen, L. Esser, B. Quinn, L. Yu, C. Yu, D. Xia, Structural basis for the quinone reduction in the  $bc_1$  complex: a comparative analysis of crystal structures of mitochondrial cytochrome  $bc_1$  with bound substrate and inhibitors at the  $Q_i$  site, *Biochemistry* 42 (2003) 9067–9080.